NUMERICAL SIMULATION OF AIDING MIXED CONVECTION IN A VERTICAL FLAT CHANNEL

Re. Zujus, R. Poskas, A. Gediminskas

Lithuanian Energy Institute, Kaunas, Lithuania

Introduction

Mixed convection investigations (the interaction of the natural and forced convection) in channels of various cross-sections and orientations are important for nuclear power technology, heat exchangers, electronic cooling systems, solar energy systems, etc. Due to the importance of the engineering applications problem, a lot of researchers concentrated their attention on the turbulent mixed convection heat transfer investigations in vertical circular tubes [1 - 3]. Wide investigations on this problem (turbulent flow in vertical channels) were performed at the Lithuanian Energy Institute [4]. Different studies showed that compared to the forced convection, heat transfer was higher in case of the opposing mixed convection (upward oriented flow due to natural convection and downward oriented flow due to forced flow). It was revealed that in case of the aiding mixed convection flows (upward oriented flow due to natural convection and upward oriented flow due to forced flow), the effectiveness of heat transfer could be seriously impaired as a result of buoyancy forces modifying the production of turbulence and laminarizing the flow. However, if higher buoyancy parameters were applied, heat transfer recovered and became even higher than the forced convection heat transfer.

Investigations of heat transfer in the laminar-turbulent transition region under the effect of buoyancy (mixed convection) were rather limited. The flow character in pipes in this region was investigated in [5, 6]. In order to visualize the flow, paint was injected in the central part of the pipe. It was reported, that the shape of the paint thread in aiding mixed convection flows with the loss of flow stability was similar to the shape of sinusoid, and the pulsation of the temperature on the pipe's wall took its place. With the increase of the buoyancy parameter, the amplitude of the paint thread sinusoid became bigger, while eventually the paint thread intermitted at the end. The initial instability of the flow depended not only on the buoyancy parameter, but also on the length of the channel (L/d). In the case of the opposing mixed convection flows, the instability of the flow was demonstrated by the appearance of the asymmetry of the paint thread just before the heating. If the buoyancy parameter increased significantly, the flow began pulsating. It was noticed that an asymmetric flow was formed inside the channel. It was also noticed in [1], that the existence of the flexure points in velocity profiles and especially the possibility of the appearance of the reversed flow, stimulated the loss of stability of laminar flow, as well as the transition to turbulent flow. The loss of stability and the transition to turbulent flow took place when $Re = Re_{cr} < 2.3 \cdot 10^3$. With the increase of Gr_q/Re, critical Reynolds number decreased. The correlation for calculation of the distance at which laminar flow loses its stability in case of the aiding mixed convection flows was suggested in [1]. In case of the opposing mixed convection flows with increasing Gr_q/Re, the flow became slower near the walls and in its core became faster. With $Gr_q/Re \approx 100$ velocity gradients became equal to zero near the wall, and with further increase of this parameter reversed flow appeared. When $Gr_q/Re \approx 170$ the instability took place, vortices appeared in the region near the wall, and then, under higher Gr_q/Re, the flow became turbulent.

The structure of the flow, in case of the opposing mixed convection, was studied in a vertical tube in [7] with moving thermocouples. After these investigations, it was concluded that at the beginning of the heating, vortices appear near the walls, which causes the fluctuation of wall temperature. As the influence of the buoyancy forces became stronger, the flow inside the channel became turbulent.

In [8] experiments (temperature and velocity fluctuations) in airflow for Re = 1000, 1300 and 1600 were performed. Flow instability in a vertical tube in case of the aiding mixed convection was analyzed. It was determined that flow loses its stability at Gr/Re > 1500.

In [9] the results on experimental and numerical investigation of the opposing mixed convection in a vertical flat channel with symmetrical heating in the laminar-turbulent transition region were presented. Numerical two-dimensional simulations were performed for the same conditions as in experiments using the Fluent code. The performed experimental investigations showed that for the higher than ambient air pressure in some Re region, heat transfer rate was more intensive than for the turbulent flow. The numerical investigations indicated that as the influence of the buoyancy became stronger, the vortical flows appeared at the wall of the channel, which caused the intensification of the heat transfer.

In this paper the results on numerical investigations of the aiding mixed convection in the laminar-turbulent transition region in the vertical flat channel are presented. Numerical three-dimensional (3D) simulations have been performed for the same channel and for the same conditions as in experiments using Ansys Fluent code. Simulations have been performed at air pressure p = 0.2 MPa with symmetrical heating for Reynolds numbers Re_{in} = 2400, 2900 and Grashof numbers Gr_{qin} = 4.1 · 10^8, 5 · 10^8 accordingly.

Methodology

In this paper the results on three-dimensional numerical modelling of aiding mixed convection in the vertical rectangular channel (height – 0.0408 m, width – 0,4 m, length – 6 m, hydrodynamic unheated length – 2.5 m, heated (calorimeter) length 3.5 m) with two-sided symmetrical heating (q_{w1} = q_{w2} = const) are presented for the steady state flow conditions in airflow. The modelling has been performed using laminar and turbulence transition models: kkl-ω [10], SST [11, 12], and Reynolds Stress ω model [13, 14].

The modelling has been carried out using Ansys Fluent code. It is a contemporary computational fluid dynamics code which is used for modelling the fluid flow and heat transfer in complex two-dimensional or three-dimensional systems [15]. This code solves the main flow and energy equations. In this case a control volume based technique is used. It is based on division of the domain into discrete control volumes using a computational grid (which at the same time describes channel geometry).

The steady state mean flow equations to be solved in the three dimensional problem are:
conservation of mass (continuity),

$$\frac{\partial(\rho u_x)}{\partial x} + \frac{\partial(\rho u_y)}{\partial y} + \frac{\partial(\rho u_z)}{\partial z} = 0 \tag{1}$$

conservation of the u_x, u_y and u_z momentum,

$$\rho u_x \frac{\partial u_x}{\partial x} + \rho u_y \frac{\partial u_x}{\partial y} + \rho u_z \frac{\partial u_x}{\partial z} = -\frac{\partial p}{\partial x} + \frac{2}{3}\frac{\partial}{\partial x}\left[\mu\left(2\frac{\partial u_x}{\partial x} - \frac{\partial u_y}{\partial y} - \frac{\partial u_z}{\partial z}\right)\right] +$$

$$+ \frac{\partial}{\partial y}\left[\mu\left(\frac{\partial u_x}{\partial y} + \frac{\partial u_y}{\partial x}\right)\right] + \frac{\partial}{\partial z}\left[\mu\left(\frac{\partial u_z}{\partial x} + \frac{\partial u_x}{\partial z}\right)\right] - \rho g_x \tag{2}$$

$$\rho u_x \frac{\partial u_y}{\partial x} + \rho u_y \frac{\partial u_y}{\partial y} + \rho u_z \frac{\partial u_y}{\partial z} = -\frac{\partial p}{\partial y} + \frac{2}{3}\frac{\partial}{\partial y}\left[\mu\left(2\frac{\partial u_y}{\partial y} - \frac{\partial u_x}{\partial x} - \frac{\partial u_z}{\partial z}\right)\right] +$$

$$+ \frac{\partial}{\partial z}\left[\mu\left(\frac{\partial u_y}{\partial z} + \frac{\partial u_z}{\partial y}\right)\right] + \frac{\partial}{\partial x}\left[\mu\left(\frac{\partial u_x}{\partial y} + \frac{\partial u_y}{\partial x}\right)\right] \tag{3}$$

$$\rho u_x \frac{\partial u_z}{\partial x} + \rho u_y \frac{\partial u_z}{\partial y} + \rho u_z \frac{\partial u_z}{\partial z} = -\frac{\partial p}{\partial z} + \frac{2}{3}\frac{\partial}{\partial z}\left[\mu\left(2\frac{\partial u_z}{\partial z} - \frac{\partial u_x}{\partial x} - \frac{\partial u_y}{\partial y}\right)\right] +$$

$$+ \frac{\partial}{\partial x}\left[\mu\left(\frac{\partial u_z}{\partial x} + \frac{\partial u_x}{\partial z}\right)\right] + \frac{\partial}{\partial y}\left[\mu\left(\frac{\partial u_y}{\partial z} + \frac{\partial u_z}{\partial y}\right)\right] \tag{4}$$

energy equation,

$$\rho u_x \frac{\partial i}{\partial x} + \rho u_y \frac{\partial i}{\partial y} + \rho u_z \frac{\partial i}{\partial z} = \frac{\partial}{\partial x}\left(\left(\frac{\mu}{Pr}\right)\frac{\partial i}{\partial x}\right) + \frac{\partial}{\partial y}\left(\left(\frac{\mu}{Pr}\right)\frac{\partial i}{\partial y}\right) + \frac{\partial}{\partial z}\left(\left(\frac{\mu}{Pr}\right)\frac{\partial i}{\partial z}\right) \tag{5}$$

The transition SST model is based on the coupling of the SST k-ω transport equations [12] with two other transport equations, one for the intermittency and one for the transition onset criteria, in terms of momentum-thickness Reynolds number.

The transition kkl-ω model is considered to be a three-equation eddy-viscosity type model, which includes transport equations for turbulent kinetic energy, laminar kinetic energy, and the inverse turbulent time scale.

The Re Stress ω model is a stress-transport model that is based on the k-ω equations [13] and LRR model [14].

Boundary conditions are:

- At the inlet to the channel longitudinal air velocity u_x is equal to inlet velocity u_{in}, transversal velocity $u_y = u_z = 0$. Air enthalpy i at the inlet to the calorimeter is equal to the inlet air enthalpy i_{in}.
- On the walls longitudinal u_x and transversal u_y, u_z velocities are equal to 0. Heat flux on the calorimeter walls (wide side walls) are $q_{w1} = q_{w2} = $ const.
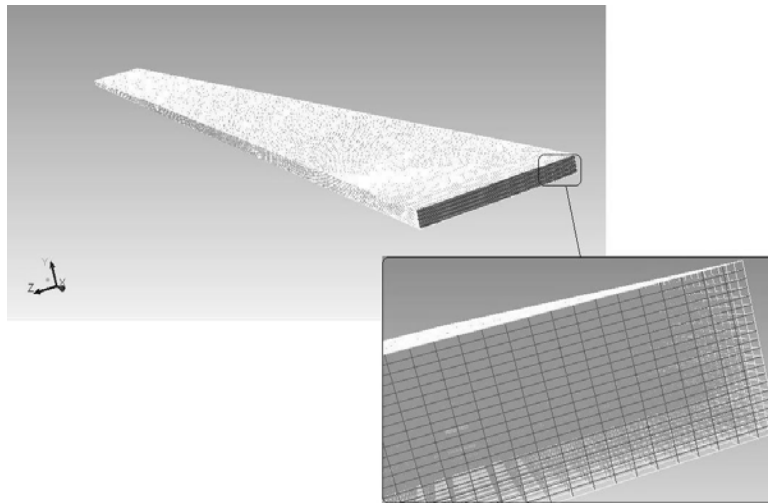

Fig. 1. Computational domain and partial view of the grid

Grid convergence study (dependence of numerical accuracy on the spatial resolution) have been performed for Re_{in} = 2900. The comparison is made among two combinations of grid density interval (1000 × 20 × 75 and 800 × 20 × 60). It was shown that the numerical accuracy is nearly independent of grid density interval within their respective ranges tested. Therefore, the spatial 1000 × 20 × 75 resolution is adopted for all the cases studied (Figure 1).

Results

The numerical investigation has been performed for two Re numbers (Re_{in} = 2400, 2900). The velocity profiles for laminar model for Re_{in} = 2400 are illustrated in Figure 2. When analyzing velocity profiles, flow developing processes can be observed. It is well known that the laminar flow has a parabolic velocity profile therefore, as the regime with such Re number is analyzed, in the hydrodynamic unheated part of the analyzed channel parabolic velocity profile is forming. The upper part (in the centre) of such profile is also visible (Fig 2 a) in the heated part of the analyzed channel at x/d_e = 0.3, but slight impact of natural convection is visible near the walls (near the walls velocity is increasing). With the increase of x/d_e, the velocity profile becomes typical to the aiding mixed convection flows i.e. near the walls velocity is higher than in the central part (M-shape velocity profile), and with increasing impact of the natural convection (for higher x/d_e), velocity is increasing near the channel walls. Moreover, in the central part at some x/d_e, velocity becomes negative and this means that reversal flow has appeared. Vortical flow is observed between 11 < x/d_e < 26, then vortexes intermit. Turbulence transition models in principle shows similar velocity profile variations along heated part of the channel, but in the case of Re Stress ω model (Fig 2 b) vortical flow is observed between 10 < x/d_e < 14, in the case of kkl-ω model (Fig 3 a) the zone of vortical flow is between 11 < x/d_e < 17 and only in the case of SST model (Fig 3 b), the vortical flow is not observed in the channel.
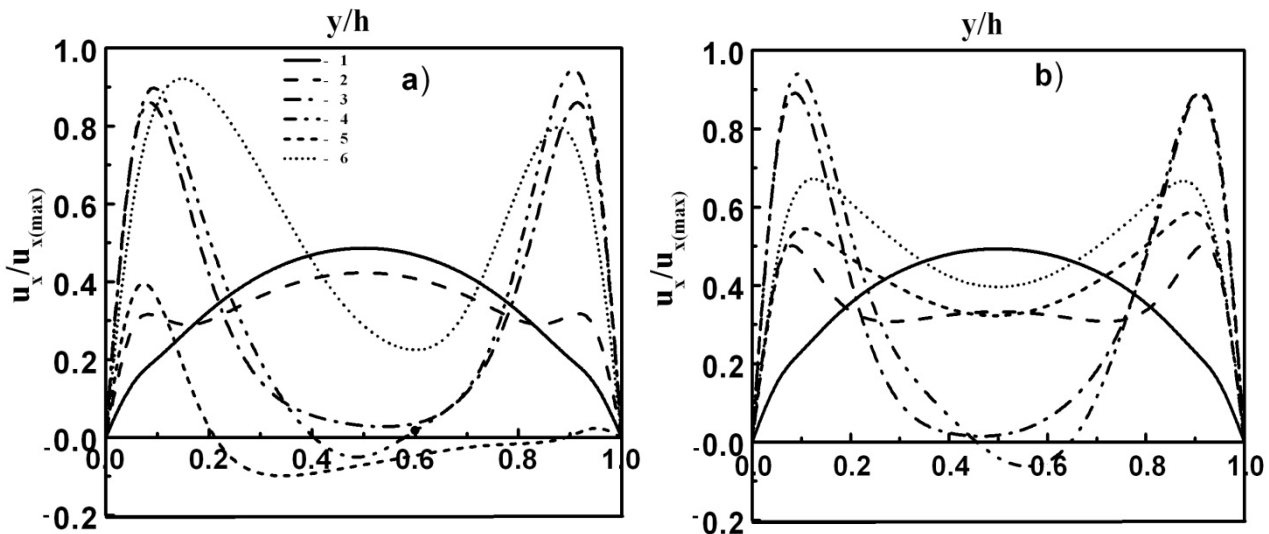

Fig. 2. The dynamics of velocity profiles for Re_{in} = 2400, $Gr_{q\,in}$ = 4.1·10^8. a) laminar; b) Re Stress ω model. 1 curve – x/d_e = 0.3; 2 – 1.9(a), 3.9(b); 3 – 10.2; 4 – 11.6(b), 12.3(a); 5 – 18.3(a), 22.3(b); 6 – 42

The performed numerical investigations for higher (Re_{in} = 2900) have shown that the dynamics of velocity profiles is similar to lower Re value (Re_{in} = 2400 Fig. 2-3), however, the vortical flow is observed only in a narrow heated part of the channel 12 < x/d_e < 14 in the case of laminar and kkl-ω models only.

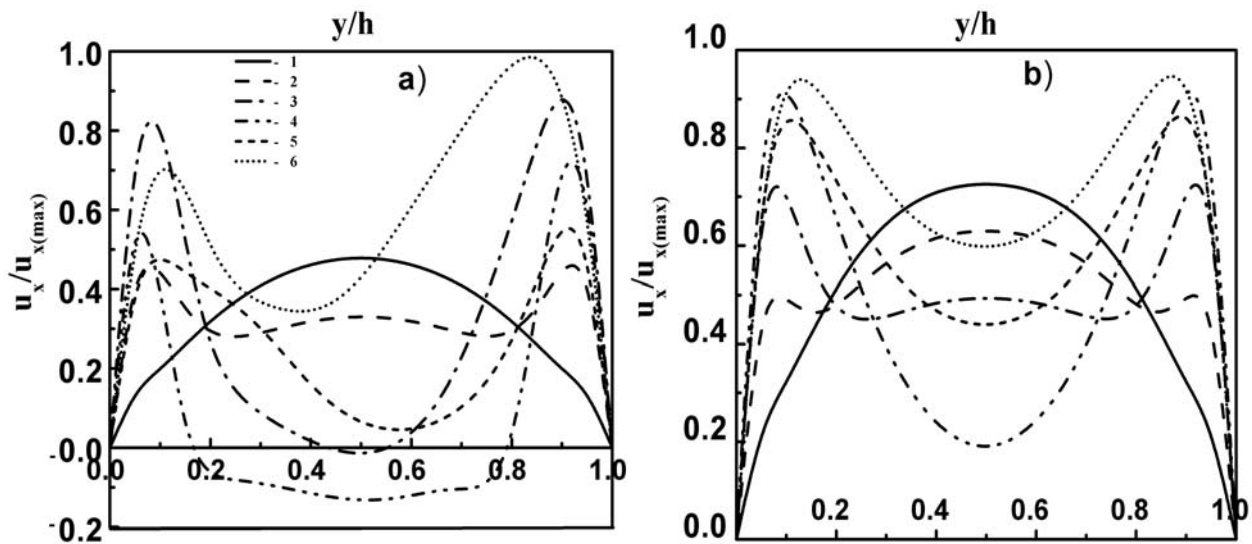Variation of heat transfer along the channel for Re_{in} = 2400 using different models is illustrated in Figure 4.

Fig. 3. The dynamics of velocity profiles for Re_{in} = 2400, $Gr_{q\,in}$ = 4.1·10^8. a) kkl-ω model; b) SST model. 1 curve – x/d_e = 0.3; 2 – 1.9(b), 3.9(a); 3 – 3.9(b), 14.2(a); 4 – 10.2(b), 15.5(a); 5 – 18.3(a), 22.3(b); 6 – 42
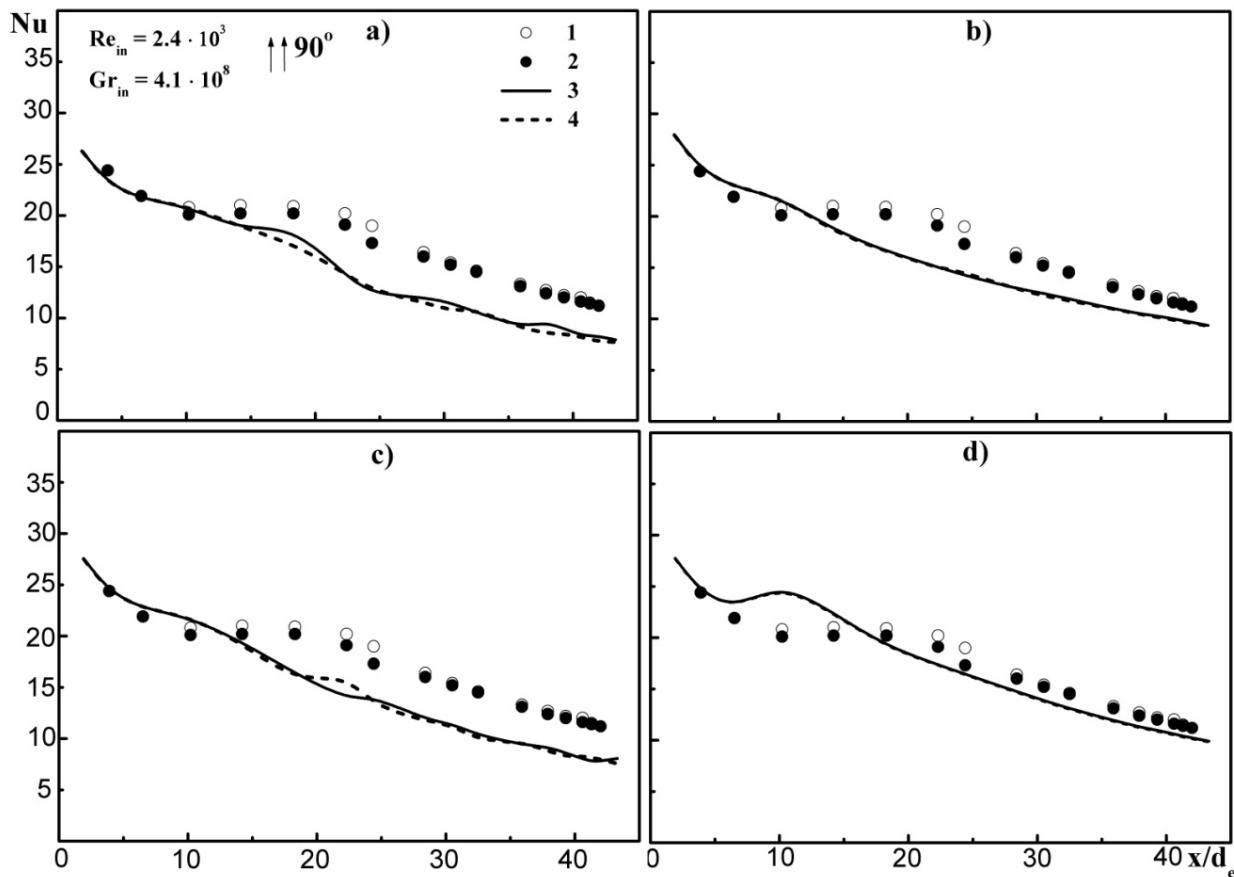

Fig. 4. Variation of heat transfer along the channel. 1 – experimental data (1 wall); 2 – experimental data (2 wall); 3 – numerical modeling results (1 wall); 4 - numerical modeling results (2 wall); a) – Laminar; b) – Re Stress ω; c) kkl-ω; d) – SST models

As it can be seen from Fig 4 a till $x/d_e \leq 10$ modeled three-dimensional heat transfer results (laminar model) coincide well with experimental data, but at $x/d_e > 10$ experimental data are higher than numerical ones and difference is till 35%. Re Stress ω model (Fig 4 b) also shows good coincidence with experiments till $x/d_e \leq 10$, but at $x/d_e > 10$ numerical results are below experiments (maximal difference is 25%). At small x/d_e ($x/d_e \leq 10$) kkl-ω model heat transfer results (Fig 4 c) also coincide well with experiments, but at $x/d_e > 10$ experimental data are higher than numerical ones and difference is till 33%. SST turbulence transition model (Fig 4 d) gives

higher Nu values till $x/d_e \leq 15$ than experimental ones, but at $x/d_e > 15$ SST model gives slightly smaller Nu values and difference is till 21%. In heat transfer stabilized region ($x/d_e = 42$) difference is about 9%). In summary it can be stated, that for smaller analyzed Re number ($Re_{in} = 2400$) the best correlation between numerical modelling results and experimental data is in case of SST model and the worst results are obtained in case of laminar model.

Heat transfer variation along the channel for larger Re number ($Re_{in} = 2900$) is shown in Figure 5. As it can be seen from Fig 5 a (laminar model) heat transfer results coincide well with experimental data only at $10 \leq x/d_e \leq 18$ and in the remaining part of the channel Nu values are smaller than experimental ones and maximal difference is 36%. Re Stress ω model Fig 5 b also shows good correlation with experiments till $x/d_e \leq 15$, but at $x/d_e > 15$ numerical results are below experiments (maximal difference is 26%). In case of kkl-ω model Fig 5 c results correlate well with experiments in large part of the channel (difference not exceeds 10%), but in some points it is quite large difference (24%). SST model results Fig 5 d shows good correlation with experiments at $24 \leq x/d_e \leq 30$ and maximal difference is 26%. So it can be stated that for $Re_{in} = 2900$ the best correlation between numerical modelling results and experimental data is noticed in case of kkl-ω model. Laminar model gives the worst correlation.
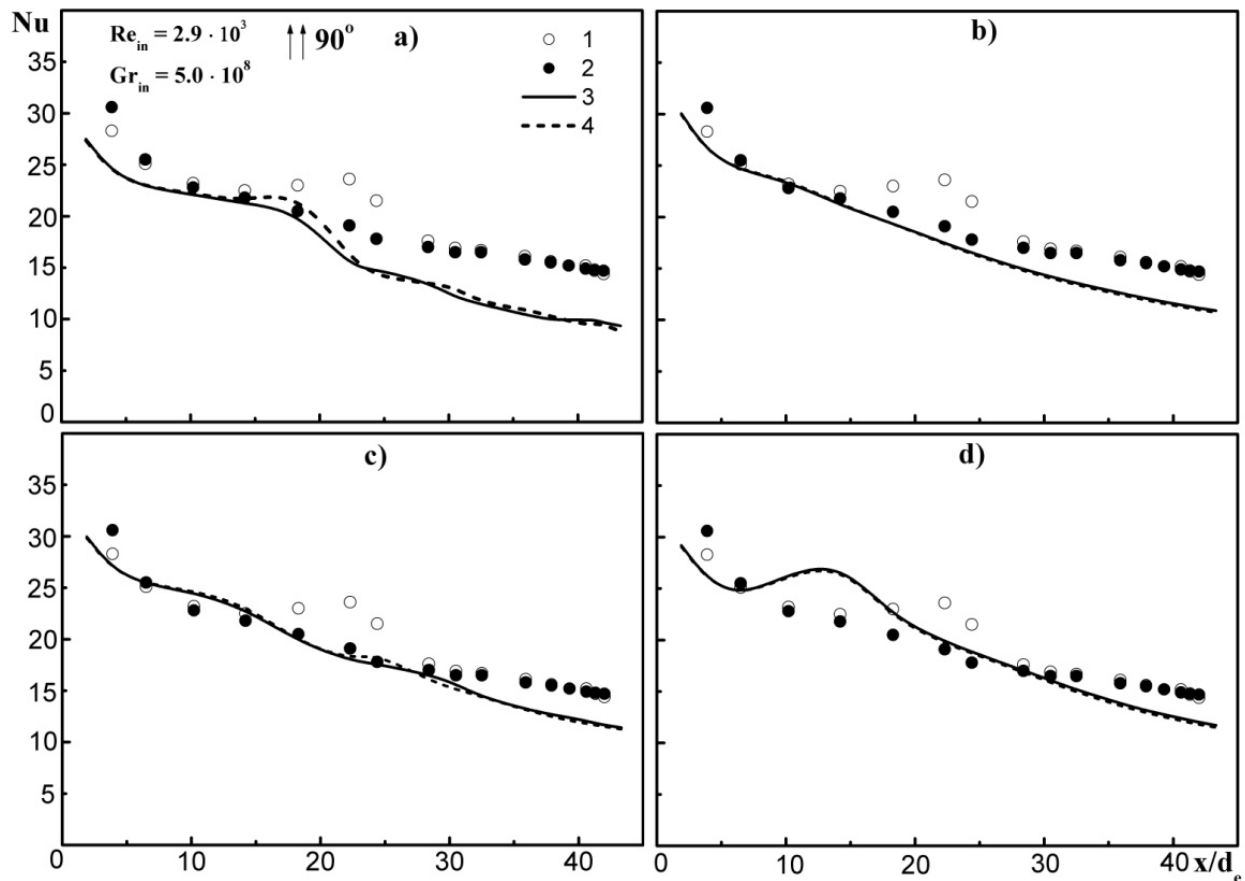

Fig. 5. Variation of heat transfer along the channel. 1 – experimental data (1 wall); 2 – experimental data (2 wall); 3 – numerical modeling results (1 wall); 4 - numerical modeling results (2 wall); a) – Laminar; b) – Re Stress ω; c) kkl-ω; d) – SST models

Conclusion

Analysis of the numerical three-dimensional simulation data on the aiding mixed convection in transition region in a vertical flat channel with symmetrical heating leads to the following conclusions:

1. Numerical modelling results for most cases (laminar and turbulence transition models) in the limited part of the thermaly developing region indicate the existence of the vortical flow that intermits later on along the channel.
2. The best correlation of the numerical modelling results with the experimental heat transfer data is obtained with the SST model for smaller analyzed Re number (Re_{in} = 2400) and with the kkl-ω transition model for higher Re number (Re_{in} = 2900).

Notation

b – channel with, m; c_p – specific heat, J/(kg·K); d_e - equivalent diameter of the channel [$d_e = 2hb/(h+b)$], m; Gr_q - Grashof number defined by the heat flux specified on the surface [$Gr_q = g·β· d_e^4·q_w/ν^2·λ$]; g - acceleration due to gravity, m/s^2; h – channel height, m; i – enthalpy, J/kg; Nu – Nusselt number [Nu = $αd_e/λ$]; Pr - Prandtl number [Pr = $μc_p/λ$]; p – pressure, Pa; q – heat flux density, W/m^2; Re - Reynolds number [Re = $ud_e/ν$]; u – local flow velocity, m/s; x – axial coordinate measured from start of heating, m; x, y ,z – coordinate; α - heat transfer coefficient; β - volumetric expansion coefficient, 1/K; λ - thermal conductivity, W/(m·K); μ - dynamic viscosity, Pa·s; $ρ$ - density, kg/m^3; subscripts: 1, 2 – first and second wall; in – at the inlet; w – at the wall.

References

1. Petukhov B. S., Polyakov A. F. Turbulent mixed convection heat transfer, Nauka, Moscow, 1986.
2. Jackson J. D., Cotton M. A; Axell B. P. Studies of mixed convection in vertical tubes. Review, International Journal of Heat Fluid Flow. 1988, Vol. 10, No. 1. pp. 2-15.
3. Jackson J. D. Influences of buoyancy on velocity, turbulence and heat transfer in ascending and descending flows in vertical passages. Proceedings of the 4th Baltic Heat Transfer Conference. Advances in Heat Transfer Engineering, Kaunas, Lithuania. 2003, pp. 57-78.
4. Vilemas J., Poškas P. Effect of body forces on turbulent heat transfer in channels, LEI-Bigell House. Kaunas-New York. 1999.
5. Scheele G. F., Rosen E. M., Hanratty T. J. Effects of Natural Convection on Transition to Turbulence in Vertical Pipes, Canadian Journal of Chemical Engineering. 1960, Vol. 38, pp. 67-73.
6. Scheele G. F., Hanratty T. J. Effects of Natural Convection Instabilities on Rates of Heat Transfer at Low Reynolds Numbers, *AIChE J.* 1963. Vol. 9, No. 2, pp. 183-185.
7. Joye D. D., Jacobs W. S. Backflow in the Inlet Region of Opposing Mixed Convection Heat Transfer in a Vertical Tube, Proceedings of the 10th International Heat Transfer Conference. 1994. Vol. 5, pp. 489-494.
8. Behzadmehr A., Laneville A., Galanis N. Experimental Study of Onset of Laminar-Turbulent Transition in Mixed Convection in a Vertical Heated Tube, International Journal of Heat and Mass Transfer, 2008. Vol. 51. No. 25-26. pp 5895–5905.
9. Poskas P., Poskas R., Sirvydas A., Smaizys A. Experimental investigation of opposing mixed convection heat transfer in the vertical flat channel in a laminar-turbulent transition region, International Journal of Heat and Mass Transfer. 2011. Vol. 54, No. 1-3, pp. 662-668.
10. Walters D. K., Cokljat D. A three-equation eddy-viscosity model for Reynolds-averaged Navier-Stokes simulations of transitional flows, Journal of Fluids Engineering. 2008, Vol. 130.
11. Menter F. R., Langtry R. B., Likki S. R., Suzen Y. B., Huang P. G., Volker S. A correlation based transition model using local variables. Part 1. Model formulation, J. of Turbomachinery. 2004. Vol. 128. No. 3. pp 413 – 422.
12. Menter F. R. Two-equation eddy-viscosity turbulence models for engineering applications, *AIAA Journal*. 1994. Vol. 32. No. 8. pp. 1598-1605.
13. Wilcox D. C. Turbulence Modeling for CFD. DCW Industries, Inc. La Canada, California. 1998

14. Launder B. E., Reece G. J. Rodi W. Progress in the development of a Reynolds-Stress turbulence closure, Journal of Fluid Mechanics. 1975. Vol. 68, No. 3. pp. 537-566.
15. ANSYS-FLUENT Inc., 2009. FLUENT 12.0 User Documentation